

# RESISTANCE SCALING ON $4N$ -CARPETS

CLAIRE CANNER, CHRISTOPHER HAYES, SHINYU HUANG, MICHAEL ORWIN, AND LUKE G. ROGERS.

ABSTRACT. The  $4N$  carpets are a class of infinitely ramified self-similar fractals with a large group of symmetries. For a  $4N$ -carpet  $F$ , let  $\{F_n\}_{n \geq 0}$  be the natural decreasing sequence of compact pre-fractal approximations with  $\cap_n F_n = F$ . On each  $F_n$ , let  $\mathcal{E}(u, v) = \int_{F_n} \nabla u \cdot \nabla v dx$  be the classical Dirichlet form and  $u_n$  be the unique harmonic function on  $F_n$  satisfying a mixed boundary value problem corresponding to assigning a constant potential between two specific subsets of the boundary. Using a method introduced by Barlow and Bass [2], we prove a resistance estimate of the following form: there is  $\rho = \rho(N) > 1$  such that  $\mathcal{E}(u_n, u_n)\rho^n$  is bounded above and below by constants independent of  $n$ . Such estimates have implications for the existence and scaling properties of Dirichlet forms on  $F$ .

## 1. INTRODUCTION

The  $4N$  carpets are a class of self-similar fractals related to the classical Sierpiński Carpets. They are defined by a finite set of similitudes with a single contraction ratio, are highly symmetric, and are post-critically infinite. Two examples, the octacarpets ( $N = 2$ ) and dodecacarpets ( $N = 3$ ) are shown in Figure 1. We do not consider the case  $N = 1$  which is simply a square.

The construction of  $4N$  carpets is as follows; illustrations for  $N = 2$  are in Figure 2. Fix  $N \geq 2$ , let  $\Lambda(N) = \{0, \dots, 4N - 1\}$  and  $C_j(N) = \exp \frac{(2j-1)i\pi}{4N} \in \mathbb{C}$ . Let  $F_0$  denote the convex hull of  $\{C_j(N), j \in \Lambda(N)\}$ . Consider contractions  $\phi_j = r(x - C_j) + C_j$  where the ratio  $r = r(N) = (1 + \cot(\pi/4N))^{-1}$  is chosen so  $\phi_j(F_0) \cap \phi_k(F_0)$  is a line segment. Let  $\Phi(x) = \cup_{j=1}^{4N} \phi_j(x)$  and  $\Phi^n$  denote the  $n$ -fold composition. Then let  $F_n = \Phi^n(F_0)$  and  $F = \cap_n F_n$  be the unique non-empty compact set such that  $\Phi(F) = F$  (see [8]). We call  $F$  the  $4N$ -carpet. Since one may verify the Moran open set condition is valid for the interior of  $F_0$ , [8, Theorem 5.3(2)] implies its Hausdorff dimension is  $d_f = -\log 4N / \log r(N) = \log 4N / \log(1 + \cot(\pi/4N))$ .

This paper is concerned by a physically-motivated problem connected to the resistance of the  $4N$  carpet, and is closely related to well-known results of Barlow and Bass [2]. To state it we need

---

2020 *Mathematics Subject Classification*. Primary: 28A80, 31C25, 31E05. Secondary: 31C15, 60J65.

*Key words and phrases*. Resistance, Fractal, Fractal carpet, Dirichlet form, Walk dimension, Spectral dimension. Work supported by NSF DMS REU 1659643.

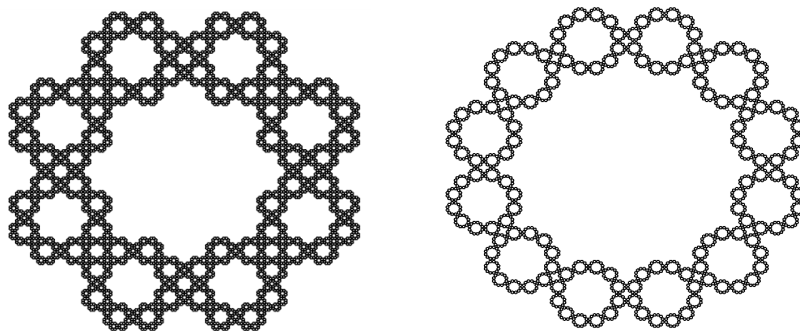


FIGURE 1. The octacarpet ( $N = 2$ ) and dodecacarpet ( $N = 3$ ) are  $4N$ -Carpets.

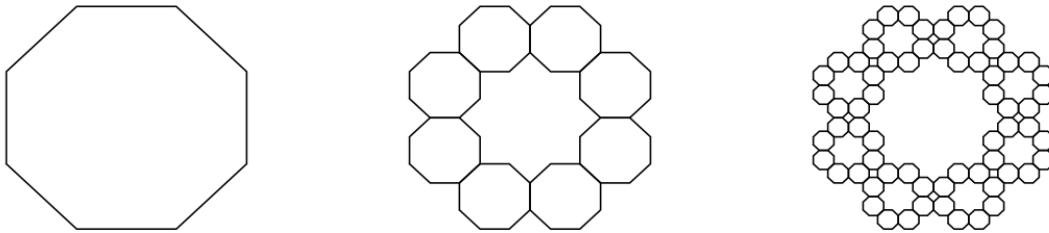


FIGURE 2. The pre-carpets  $F_0$ ,  $F_1$  and  $F_2$  for the octacarpet ( $N = 2$ ).

some further notation. Writing subindices modulo  $4N$ , let  $L_j$  be the line segment from  $C_j$  to  $C_{j+1}$  (these are shown for the case  $N = 2$  in the left diagram in Figure 5). Then define

$$(1.1) \quad A_n = F_n \cap \left( \bigcup_{k=0}^{N-1} L_{4k} \right) \quad B_n = F_n \cap \left( \bigcup_{k=0}^{N-1} L_{4k+2} \right)$$

Supposing  $F_n$  to be constructed from a thin, electrically conductive sheet let  $R_n = R_n(N)$  be the effective resistance (as defined in (2.2) below) when the edges of  $A_n$  are short-circuited at potential 1 and those of  $B_n$  are short-circuited at potential 0. Bounds for  $R_n$  have a well-known connection to exit time estimates for Brownian motion and to proving the existence of and obtaining bounds for the “spectral dimension” of  $F$ , as in [3]; they also play a significant role in the Barlow-Bass proof of the existence of Brownian motion on the Sierpiński Carpet and bounds on the associated heat kernel. Although the present work generalizes [2] to the  $4N$ -carpets, we do not establish the existence of a Brownian motion. In this connection, we note that the PhD thesis or Ulysses Andrews [1] establishes existence of a Brownian motion on  $4N$ -carpets by the Barlow-Bass method under certain assumptions, one of which is that there is a resistance estimate like that in Theorem 1.1. Our main result is the following theorem.

**Theorem 1.1.** *For fixed  $N \geq 2$  there is a constant  $\rho = \rho(N)$  such that  $\frac{9}{44N} R_0 \rho^n \leq R_n \leq \frac{44N}{9} R_0 \rho^n$ .*

*Proof.* The majority of the work is to establish (in Theorem 4.1 below) that there are constants  $c, C$  so  $cR_n R_m \leq R_{n+m} \leq CR_n R_m$ . Then  $S_n = \log cR_n$  is superadditive and  $S'_n = \log CR_n$  is subadditive, so Fekete’s lemma implies  $\frac{1}{n} S_n \rightarrow \sup \frac{1}{n} S_n$  and  $\frac{1}{n} S'_n \rightarrow \inf \frac{1}{n} S'_n$ . However  $\frac{1}{n} (S_n - S'_n) \rightarrow 0$ , so defining  $\log \rho$  to be the common limit we conclude  $\frac{1}{n} S_n \leq \log \rho \leq \frac{1}{n} S'_n$  and thus  $cR_n \leq \rho^n \leq CR_n$ . The constants  $c$  and  $C$  in the stated bound are those from Theorem 4.1.  $\square$

## 2. RESISTANCE, FLOWS AND CURRENTS

We recall some necessary notions regarding Dirichlet forms on graphs and on Lipschitz domains. Our treatment closely follows [2], which in turn refers to [5] for the graph case.

**2.1. Graphs.** On a finite set of points  $G$  suppose we have  $g : G \times G \rightarrow \mathbb{R}$  satisfying for all  $x, y \in G$  that  $g(x, y) = g(y, x)$ ,  $g(x, y) \geq 0$  and  $g(x, x) = 0$ . We call  $g$  a conductance. It defines a Dirichlet form by

$$\mathcal{E}_G(u, u) = \frac{1}{2} \sum_{x \in G} \sum_{y \in G} g(x, y) (u(x) - u(y))^2.$$

For disjoint subsets  $A, B$  from  $G$  the effective resistance between them is  $R_G(A, B)$  defined by

$$(2.1) \quad R_G(A, B)^{-1} = \inf \{ \mathcal{E}_G(u, u) : u|_A = 0, u|_B = 1 \}.$$

The set of functions in (2.1) are called feasible potentials and the infimum is attained at a unique such potential  $\tilde{u}_G$ .

A current from  $A$  to  $B$  is a function  $I$  on the edges of the conductance graph, meaning  $I : \{x, y : g(x, y) > 0\} \rightarrow \mathbb{R}$ , with properties:  $I(x, y) = -I(y, x)$  for all  $x, y$  and  $\sum_{y \in G} I(x, y) = 0$  if  $x \notin A \cup B$ . It is called a feasible current if it has unit flux, meaning  $\sum_{x \in B} \sum_{y \in G} I(x, y) =$

$-\sum_{x \in A} \sum_{y \in G} I(x, y) = 1$ . Note that the first equality is a consequence of the definition of a current. The energy of the current is defined by

$$E_G(I, I) = \frac{1}{2} \sum_{x \in G} \sum_{y \in G} g(x, y)^{-1} I(x, y)^2.$$

**Theorem 2.1** ([5, Section 1.3.5]).

$$R_G(A, B) = \inf\{E_G(I, I) : I \text{ is a feasible current}\}.$$

This well-known result is proven by showing that for the optimal potential  $\tilde{u}_G$  one may define a current by  $\nabla u_G(x, y) = (\tilde{u}_G(y) - \tilde{u}_G(x))g(x, y)$ , this current has flux  $R_G(A, B)^{-1}$  and the optimal current which attains the infimum in the theorem is  $\tilde{I}_G = R_G(A, B)\nabla\tilde{u}_G$ .

**2.2. Lipschitz domains.** The corresponding quantities on a Lipschitz domain  $\Omega \subset \mathbb{C}$  may be defined as follows. Suppose  $A, B$  are disjoint closed subsets of  $\partial\Omega$ , write  $\sigma$  for the surface measure on  $\partial\Omega$  and  $\nu$  for the interior unit normal. For  $u \in C(\bar{\Omega}) \cap H^1(\Omega)$ , the latter being the Sobolev space with one derivative in  $L^2$ , let  $\mathcal{E}_\Omega(u, u) = \int_\Omega |\nabla u|^2$  and call  $u$  a feasible potential if  $u|_A = 0$  and  $u|_B = 1$ . Then define the effective resistance by

$$(2.2) \quad R_\Omega(A, B)^{-1} = \inf\{\mathcal{E}_\Omega(u, u) : u \text{ is a feasible potential}\}.$$

Now consider a vector field  $J : \Omega \rightarrow \mathbb{R}^2$ .  $J$  is a current between  $A$  and  $B$  if  $J \in BV(\Omega)$  with  $\nabla \cdot J = 0$  on  $\Omega$  in the sense of distributions and  $J \cdot \nu = 0$   $\sigma$ -a.e. on  $\partial\Omega \setminus (A \cup B)$ . The quantity  $\int_A J \cdot \nu d\sigma$  is called the flux through  $A$  and the condition  $\nabla \cdot J = 0$  and a Gauss-Green integration (e.g. using [6, Theorem 1 of Section 5.8]) gives  $\int_B J \cdot \nu d\sigma = -\int_A J \cdot \nu d\sigma$ . The current is feasible if both of these fluxes equal 1. Our work here depends crucially on the following result, for which we refer to [4]. It should be noted that this result is not valid for arbitrary mixed boundary value problems on Lipschitz domains; in particular, in [4] it is required that the pieces of the boundary on which the Dirichlet and Neumann conditions hold meet at an angle less than  $\pi$ . This condition will be true for our sets. Alternatively, one can note that our sets have polygonal boundary and therefore the analysis of Grisvard [7, Section 4.3.1] is applicable.

**Theorem 2.2.** *For the choices of domain  $\Omega$  and sets  $A, B$  considered in this paper, there is a unique  $\tilde{u}_\Omega \in C(\bar{\Omega}) \cap H^1(\Omega)$  with  $\nabla\tilde{u}_\Omega \in L^2(d\sigma)$  which solves the mixed boundary value problem*

$$\begin{cases} \Delta\tilde{u}_\Omega = 0 \text{ in } \Omega \\ \tilde{u}_\Omega|_A = 0, \tilde{u}_\Omega|_B = 1 \\ \frac{\partial\tilde{u}_\Omega}{\partial\nu} = 0 \text{ a.e. } d\sigma \text{ on } \partial\Omega \setminus (A \cup B). \end{cases}$$

Once this is known, the arguments in [2] directly translate to yield the following analogue of the previously stated result for graphs. It is perhaps worth remarking that the argument uses that  $\nabla\tilde{u}_\Omega$  is a current, which requires more regularity on the interior of  $\Omega$  than simply  $\tilde{u}_\Omega \in H^1(\Omega)$ , but the required regularity is immediate from  $\Delta\tilde{u} = 0$  on  $\Omega$ .

**Theorem 2.3** (See [2, Proposition 2.2 and Theorem 2.3]). *The function  $\tilde{u}_\Omega$  from Theorem 2.2 is the unique minimizer of (2.2) so satisfies  $R_\Omega(A, B)^{-1} = \mathcal{E}_\Omega(\tilde{u}_\Omega, \tilde{u}_\Omega)$ . Moreover  $\tilde{J}_\Omega = R_\Omega(A, B)\nabla\tilde{u}_\Omega$  is the unique minimizer for  $\inf\{E_\Omega(J, J) : J \text{ is a feasible current}\}$  and thus  $E_\Omega(\tilde{J}_\Omega, \tilde{J}_\Omega) = R_\Omega(A, B)$ .*

### 3. RESISTANCE ESTIMATES

Suppose Theorem 2.2 is applicable to the Lipschitz domain  $\Omega$  and disjoint subsets  $A, B \subset \partial\Omega$ . In light of (2.2) we can bound the resistance from below by  $\mathcal{E}_\Omega(u, u)^{-1}$  for  $u$  a feasible potential, and by the characterization in Theorem 2.3 we can bound the resistance from above by  $E_\Omega(J, J)$  for  $J$  a feasible current. To get good resistance estimates one must ensure the potential and current give comparable bounds.

We do this for the pre-carpet sets  $F_{m+n}$  following the method of Barlow and Bass in [2]. First we define graphs  $G_m$  and  $D_m$ , which correspond to scale  $m$  approximations of a current and potential (respectively) on  $F_m$ , and for which the resistances are comparable. Next we establish the key technical step, which involves using the symmetries of the  $4N$  gasket to construct a current with prescribed fluxes through certain sides  $L_j \cap F_n$  from the optimal current on  $F_n$  (see Proposition 3.8), and to construct a potential with prescribed data at the endpoints of these sides from the optimal potential on  $F_n$  (see Proposition 3.10). Combining these results we establish the resistance bounds in Theorem 4.1 by showing that the optimal current on  $G_m$  can be used to define a current on  $F_{m+n}$  with comparable energy, and the optimal potential on  $D_m$  can be used to define a potential on  $F_{m+n}$  with comparable energy.

The two symmetries of  $F$  and the pre-carpets  $F_n$  that play an essential role are the rotation  $\theta(z) = ze^{i\pi/2N}$  and complex conjugation. They preserve  $F$  and all  $F_n$ .

**3.1. Graph approximations.** For a fixed  $m$  the pre-carpet  $F_m$  is a union of cells, each of which is a scaled translated copy of the convex set  $F_0$ . We define graphs that reflect the adjacency structure of the cells.

In  $F_1$ , we refer to a cell by the unique vertex  $C_j$  it contains. Focusing on the  $C_0$  cell, we identify three sides of significance: the side contained in  $L_0$ , and the sides where the  $C_0$  cell meets the  $C_{\pm 1}$  cells. By symmetry under complex conjugation the side where the  $C_0$  and  $C_1$  cells meet is on the real axis. This common side is mapped to the intersection of the  $C_0$  and  $C_{-1}$  cells by the rotation  $\theta^{-1}$ . Recalling the contraction  $\phi_0$  which maps  $F_0$  to the  $C_0$  cell we conclude that these sides of the  $C_0$  cell are  $\phi_0(L_0)$ ,  $\phi_0(L_N)$  and  $\phi_0(L_{3N-1})$ .

It is straightforward to find a map  $\psi_j$  which takes  $F_0$  to the  $C_j$  cell in  $F_1$  and has the same adjacency properties we had for the  $C_0$  cell, specifically that  $\psi_j(L_0) \subset A_1 \cup B_1$ , while  $\psi_j(L_N)$  and  $\psi_j(L_{3N-1})$  are the sides where the  $C_j$  cell intersects the  $C_{j\pm 1}$  cells. Using symmetry under complex conjugation and the rotation  $\theta$ , we see this is achieved by setting

$$\psi_j(z) = \begin{cases} \phi_j \circ \theta^j(z) & \text{if } j \equiv 0 \pmod{2} \\ \phi_j \circ \theta^{j-1}(\bar{z}) & \text{if } j \equiv 1 \pmod{2}. \end{cases}$$

and we also define  $\Psi_0 = \cup_j \psi_j : F_0 \rightarrow F_1$ .

Observe that for the cells in  $F_1$  we mapped  $L_0$  to the sides of  $A_1 \cup B_1$  because these are the sides on which we should specify a voltage or current for our resistance problem. At subsequent levels of the construction things are slightly different. Fix a level  $m$  cell and consider mapping  $F_0$  to a level  $m+1$  cell within it. As before we arrange that the sides  $L_N$  and  $L_{3N-1}$  are mapped to the places where the level  $m+1$  cells meet their neighbors of the same size. However there can also be adjacency where the level  $m$  cell meets its neighbors. Six level  $m+1$  cells each contain a single side where there is adjacency to a cell outside their parent  $m$  cell, and we want each of these sides to be the image of  $L_0$  under the map of  $F_0$  to the corresponding cell. For other  $m+1$  cells we do not care which side is the image of  $L_0$ .

Since the preceding problem involves only scales  $m$  and  $m+1$  we define the maps as though  $m=0$ . In this case the required condition is that for each  $j$  one has a map  $\tilde{\psi}_j$  from  $F_0$  to the  $C_j$  cell of  $F_1$  under which  $\tilde{\psi}_j(L_N)$  and  $\tilde{\psi}_j(L_{3N-1})$  are the sides where the  $C_j$  cell intersects the  $C_{j\pm 1}$  cells. In addition one wants  $\tilde{\psi}_j(L_0) \subset L_0$  if  $j \in \{0, 1\}$ ,  $\tilde{\psi}_j(L_0) \subset L_N$  if  $j \in \{N, N+1\}$  and  $\tilde{\psi}_j(L_0) \subset L_{3N-1}$  if  $j \in \{3N-1, 3N\}$ . If  $N$  is even then  $\tilde{\psi}_j = \psi_j$  already has these properties unless  $j \in \{3N-1, 3N\}$  where we put  $\tilde{\psi}_{3N-1}(z) = \phi_{3N-1} \circ \theta^{3N-1}(z)$  and  $\tilde{\psi}_{3N}(z) = \phi_{3N} \circ \theta^{3N-1}(\bar{z})$ . Similarly, if  $N$  is odd we set  $\tilde{\psi}_j = \psi_j$  unless  $j \in \{N, N+1\}$  in which case we define  $\tilde{\psi}_N(z) = \phi_N \circ \theta^N(z)$  and  $\tilde{\psi}_{N+1}(z) = \phi_{N+1} \circ \theta^N(\bar{z})$ .

Finally, for a length  $m$  word  $w = j_1 j_2 \cdots j_m$  we put  $\psi_w = \psi_{j_1} \circ \tilde{\psi}_{j_2} \circ \cdots \circ \tilde{\psi}_{j_m}$  and define a map  $\Psi_m = \cup_{|w|=m} \psi_w : F_0 \rightarrow F_m$ .

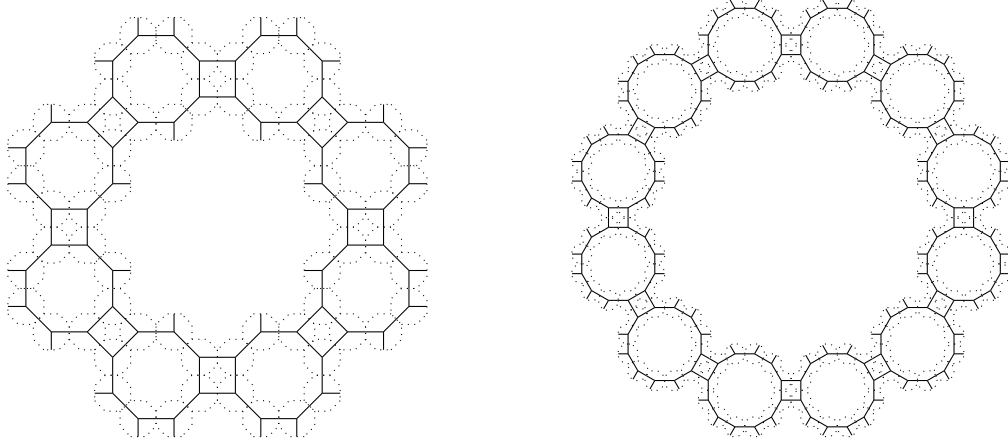


FIGURE 3. The graph approximations  $G_2$  for the octacarpet ( $N = 2$ ) and the dodecacarpet ( $N = 3$ ).

We can now define the graphs  $G_m$  that we will use to approximate currents on  $F_m$ . They correspond to ignoring the internal structure of cells and recording only the (net) flux through the intersections of pairs of cells. Figure 3 shows such graphs for  $n = 2$  on the octacarpet and dodecacarpet.

**Definition 3.1.** The graph  $G_0$  has vertices at 0 (the center of  $F_0$ ) and at  $\frac{1}{2}(C_j + C_{j+1})$  for  $j = 0, N, 3N - 1$  (which are the midpoints of the sides  $L_0 \cap F_0$ ,  $L_N \cap F_0$  and  $L_{3N-1} \cap F_0$ ). It has one edge from 0 to each of the other three vertices. The graphs  $G_m$  are defined via  $G_m = \Psi_m(G_0)$ .

Let  $\tilde{I}_m^G$  be the optimal current from  $A_m$  to  $B_m$  on  $G_m$ ; by symmetry the flux through each vertex in  $A_m$  is then  $-\frac{2}{N}$  and that through each vertex in  $B_m$  is  $\frac{2}{N}$ , giving unit flux from  $A_m$  to  $B_m$ ; these sets were defined in (1.1). The corresponding optimal potential is denoted  $\tilde{u}_m^G$  and is 0 on  $A_m$  and 1 on  $B_m$ . We write  $R_m^G$  for the resistance of  $G_m$  defined as in (2.1). Also note that  $\tilde{I}_m^G \circ \psi_w$  is a current on  $G_0$  for each word  $w$  of length  $m$ .

The graphs  $D_m$  that we use to approximate potentials on  $F_m$  have vertices at each endpoint of a side common to two cells. Figure 4 shows the first few  $D_n$  for  $N = 2$  and  $N = 3$ .

**Definition 3.2.** The graph  $D_0$  has vertices  $\{0, C_0, C_1, C_N, C_{N+1}, C_{3N-1}, C_{3N}\}$  and edges from 0 to each of the other six vertices. The graphs  $D_m$  are defined by  $\Psi_m(D_0)$ . Figure 4 shows these graphs for  $n = 0, 1, 2$  on the octacarpet and dodecacarpet.

We let  $\tilde{u}_m^G$  denote the optimal potential on  $D_m$  for the boundary conditions  $\tilde{u}_m = 0$  at vertices in  $A_m$  and  $\tilde{u}_m = 1$  at vertices in  $B_m$ . The resistance of  $D_m$  is written  $R_m^D$ . As for currents,  $\tilde{u}_m \circ \psi_w$  is a potential on  $D_0$  for any word  $w$  of length  $m$ .

**Lemma 3.3.** For all  $m \geq 1$ ,  $R_m^G = 2R_m^D$ .

*Proof.* Each edge in  $G_m$  connects the center  $x$  of a cell to a point  $y$  on a side of the cell. Writing  $y_{\pm}$  for the endpoints of that side we see that there are two edges in  $D_m$  connecting  $x$  to the same side at  $y_{\pm}$ . In this sense, each edge of  $G_m$  corresponds to two edges of  $D_m$  and conversely.

From the optimal potential  $\tilde{u}_m^G$  for  $G_m$  define a function  $f$  on  $D_m$  by setting  $f(x) = \tilde{u}_m^G(x)$  at cell centers and  $f(y_{\pm}) = \tilde{u}_m^G(y)$  at endpoints  $y_{\pm}$  of a side with center  $y$ . This ensures  $f(y_{\pm}) - f(x) = \tilde{u}_m^G(y) - \tilde{u}_m^G(x) = \tilde{u}_m^G(y) - \tilde{u}_m^G(x)$ , so that two edges in  $D_m$  have the same edge difference as the corresponding single edge in  $G_m$ . Clearly  $f$  is a feasible potential on  $D_m$ , so  $(R_m^D)^{-1} \leq \mathcal{E}_{D_m}(f, f) = 2\mathcal{E}_{G_m}(\tilde{u}_m^G, \tilde{u}_m^G) = 2(R_m^G)^{-1}$ .

Conversely, beginning with the optimal potential  $\tilde{u}_m^D$  define  $f$  on  $G_m$  by  $f(x) = \tilde{u}_m^D(x)$  at cell centers and  $f(y) = \frac{1}{2}(\tilde{u}_m^D(y_+) + \tilde{u}_m^D(y_-))$  if  $y$  is the center of a cell side with endpoints  $y_{\pm}$ . The edge

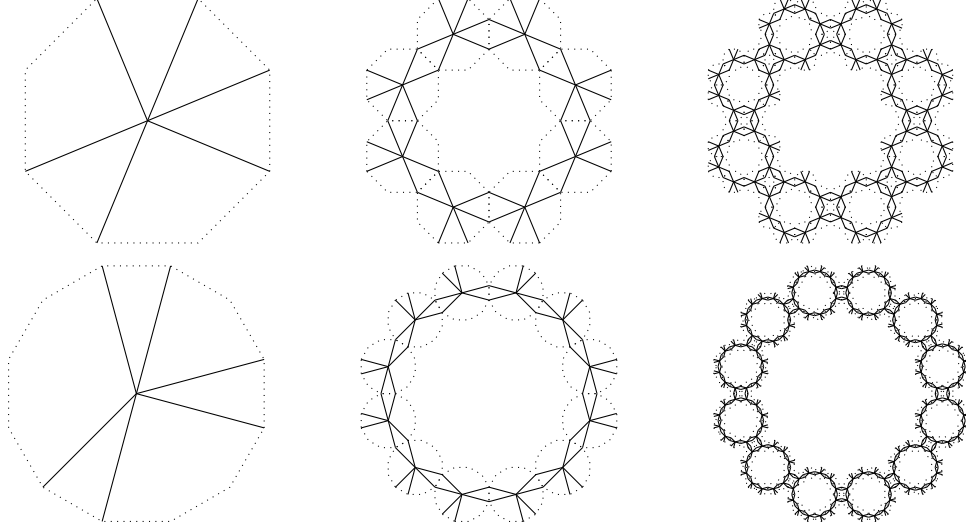


FIGURE 4. The graph approximations  $D_0$ ,  $D_1$  and  $D_2$  for the octacarpet ( $N = 2$ ) and the dodecacarpet ( $N = 3$ ). Note that  $D_0$  corresponds with the sides  $L_0$ ,  $L_N$ , and  $L_{3N-1}$ , whereas  $D_1, D_2$  correspond with  $A_1 \cup B_1$  and  $A_2 \cup B_2$ .

difference  $f(x) - f(y)$  in  $G_m$  is half the sum of the edge difference on the corresponding edges in  $D_m$ , so using that  $f$  is a feasible potential on  $G_m$  we have  $(R_m^G)^{-1} \leq \mathcal{E}_{G_m}(f, f) = \frac{1}{2} \mathcal{E}_{D_m}(\tilde{u}_m^G, \tilde{u}_m^G) = \frac{1}{2} (R_m^D)^{-1}$ .  $\square$

**3.2. Currents and potentials with energy estimates via symmetry.** Fix  $n \geq 0$  and recall that  $\tilde{u}_{F_n}$  denotes the optimal potential on  $F_n$  with boundary values 0 on  $A_n$  and 1 on  $B_n$ . In order to exploit the symmetries of  $F_n$  it is convenient to work instead with  $u_n = 2\tilde{u}_{F_n} - 1$ ; evidently  $\mathcal{E}_{F_n}(u_n, u_n) = 4\mathcal{E}_{F_n}(\tilde{u}_{F_n}, \tilde{u}_{F_n}) = 4R_n^{-1}$  is then minimal for potentials that are  $-1$  on  $A_n$  and  $1$  on  $B_n$ . The corresponding current  $J_n = R_n \nabla u_n$  minimizes the energy for currents with flux 2 from  $A_n$  to  $B_n$  and has  $E_{F_n}(J_n, J_n) = 4R_n$ . We begin our analysis by recording some symmetry properties of  $J_n$ .

**Lemma 3.4.** *Both  $u_n \circ \theta^2 = -u_n$  and  $J_n \circ \theta^2 = -J_n$ .*

*Proof.* The rotation  $\theta$  takes  $C_j$  to  $C_{j+1}$ , thus  $L_j$  to  $L_{j+1}$ . It then follows from the definition (1.1) of  $A_n$  and  $B_n$  that  $\theta^2$  exchanges  $A_n$  and  $B_n$ . Since the optimal potential  $u_n$  and current  $J_n$  are determined by their boundary data on  $A_n$  and  $B_n$  this gives the result.  $\square$

One consequence of this lemma is that the flux of  $J_n$  through each of the sides  $L_j \cap F_n$  in  $A_n$  is independent of  $j$  and hence equal to  $-\frac{2}{N}$ . Similarly, the flux through each side in  $B_n$  is  $\frac{2}{N}$ .

**Lemma 3.5.** *Both  $u_n(\bar{z}) = u_n(z)$  and  $J_n(\bar{z}) = J_n(z)$ .*

*Proof.* Under complex conjugation the point  $C_j = \exp \frac{(2j-1)i\pi}{4N}$  is mapped to

$$\bar{C}_j = \exp \frac{(1-2j)i\pi}{4N} = \exp \frac{(8N-2j+1)i\pi}{4N} = \exp \frac{(2(4N-j+1)-1)i\pi}{4N} = C_{4N-j+1}$$

Then the endpoints  $C_{4k}$  and  $C_{4k+1}$  of  $L_{4k}$  are mapped to  $C_{4(N-k)+1}$  and  $C_{4(N-k)}$  so  $L_{4k}$  is mapped to  $L_{4(N-k)}$ . This shows  $A_n$  is invariant under complex conjugation. Similarly,  $\bar{C}_{4k+2} = C_{4(N-k-1)+3}$  and  $\bar{C}_{4k+3} = C_{4(N-k-1)+2}$ , so  $L_{4k+2}$  is mapped to  $L_{4(N-k-1)}$  and  $B_n$  is invariant under complex conjugation. Both  $u_n$  and  $J_n$  are determined by their boundary data on these sets.  $\square$

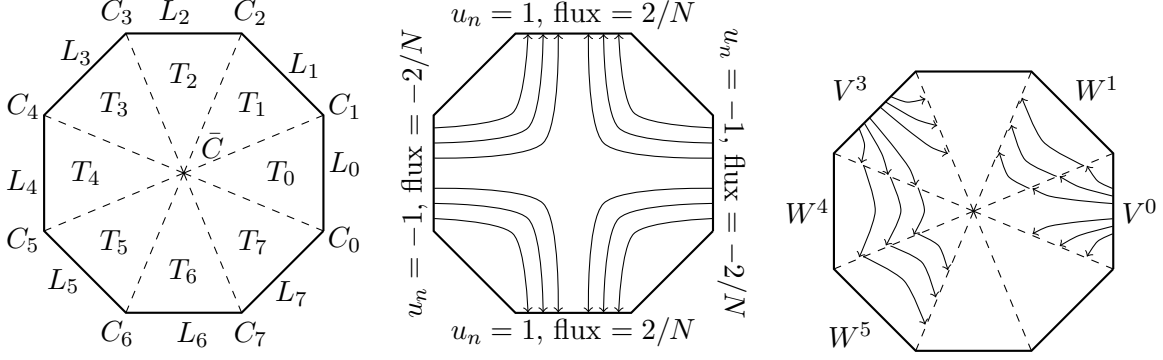


FIGURE 5. For  $N = 2$ : Decomposition of  $F_0$  into triangles  $T_j$  (left), General current flow lines for  $J_n$  (middle), and examples of  $V^j$  and  $W^j$  vector fields (right)

We decompose  $F_n$  into triangles by taking, for integers  $j$  and  $j + 1$  modulo  $4N$ ,  $T_j$  to be the interior of the triangle with vertices  $\{0, C_j, C_{j+1}\}$ . This is shown for  $N = 2$  in the left image in Figure 5. Then the central diagram in Figure 5 illustrates the fact that, up to a change of sign, both  $u_n$  and  $J_n$  have one behavior on triangles  $T_j$  with  $j$  even, and another behavior on triangles with  $j$  odd. This motivates us to define

$$(3.1) \quad v^j = (u_n \circ \theta^{-j})|_{T_j} \quad w^j = (u_n \circ \theta^{-j+1})|_{T_j}$$

$$(3.2) \quad V^j = (J_n \circ \theta^{-j})|_{T_j} \quad W^j = (J_n \circ \theta^{-j+1})|_{T_j}.$$

Examples of  $V^j$  and  $W^j$  on triangles  $T_1$  and  $T_4$  are shown on the right in Figure 5 for  $N = 2$ .

Symmetry under rotations shows us that the following quantities are independent of  $j$

$$(3.3) \quad \mathcal{E}_n(v) = \int_{T_j} |v^j|^2 \quad \mathcal{E}_n(w) = \int_{T_j} |w^j|^2$$

$$(3.4) \quad E_n(V) = \int_{T_j} |V^j|^2 \quad E_n(W) = \int_{T_j} |W^j|^2$$

and therefore that

$$(3.5) \quad 4R_n^{-1} = \mathcal{E}_{F_n}(u_n, u_n) = 2N(\mathcal{E}_n(v) + \mathcal{E}_n(w))$$

$$(3.6) \quad 4R_n = E_{F_n}(J_n, J_n) = 2N(E_n(V) + E_n(W)).$$

**Lemma 3.6.** For any  $j \in \Lambda(N)$ ,  $\int_{T_j} \nabla v^j \cdot \nabla w^j = \int_{T_j} V^j \cdot W^j = 0$ .

*Proof.* By rotational symmetry it is enough to verify this for  $j = 0$ . Since  $J_n = R_n u_n$ , we have  $\nabla v^j = R_n V^j$  and  $\nabla w^j = R_n W^j$ , so we work only with  $V^0$  and  $W^0$ . The triangle  $T_0$  is symmetrical under complex conjugation, and using Lemmas 3.4 and 3.5 we have

$$(3.7) \quad V^0(\bar{z}) = J_n(\bar{z}) = J_n(z) = V^0(z),$$

$$(3.8) \quad W^0(\bar{z}) = J_n \circ \theta(\bar{z}) = -J_n \circ \theta^{-1}(\bar{z}) = -J_n(\overline{\theta(z)}) = -J_n(\theta(z)) = -W^0(z).$$

Thus  $V^0 \cdot W^0(\bar{z}) = -V^0 \cdot W^0(z)$  and the result follows.  $\square$

In addition to being orthogonal, the vector fields  $V^j$  and  $W^j$  have the property that they can easily be glued together to form currents on  $F_n$ . Recall that to be a current a vector field  $J$  of bounded variation must have  $\nabla \cdot J = 0$ .

**Lemma 3.7.** If  $J$  is a vector field such that  $J|_{T_l} = \alpha_l V^l + \beta_l W^l$  and  $\alpha_{l+1} + \alpha_l = \beta_{l+1} - \beta_l$  for each  $l$ , then  $J$  is a current.

*Proof.* The fields  $V^l$  and  $W^l$  are currents, so are of bounded variation and zero divergence on  $T_l$ . It follows that the field is of bounded variation on  $F_n$  by the argument of [6, Theorem 1 of Section 5.4]. Moreover, a small modification of the proof of that theorem, together with the Gauss-Green theorem [6, Theorem 1 of Section 5.8] shows that the divergence on the radial line common to the boundaries of  $T_l$  and  $T_{l+1}$  is the sum of the oriented fluxes through these surfaces, times the linear measure. It is perhaps worth noting that since  $T_l$  and  $T_{l+1}$  are open, the fields are actually not defined (pointwise) on this common side, but this is of no significance because they are distributions.

The symmetry of  $V^0$  in (3.7) shows the fluxes of  $V^0$  and  $-V^1$  cancel on  $T_0 \cap T_1$ , so  $V^0 - V^1$  is a current on  $T_0 \cup T_1$ . Similarly, the antisymmetry of  $W^0$  in (3.8) shows the fluxes of  $W^0$  and  $W^1$  cancel on  $T_0 \cap T_1$ , so  $W^0 + W^1$  is a current on  $T_0 \cup T_1$ . In addition we note that  $V^1 + W^1 = J_n|_{T_0 \cup T_1}$  is the restriction of the optimal current and is hence a current on  $T_0 \cup T_1$ . Combining these with the definition (3.2) we see that each of  $V^l - V^{l+1}$ ,  $W^l + W^{l+1}$  and  $V^l + W^{l+1}$  are currents on  $T_l \cup T_{l+1}$  as they are obtained from the  $l = 0$  case by rotations.

The divergence of  $J$  then vanishes on  $T_l \cap T_{l+1}$  by writing  $J|_{T_l \cup T_{l+1}}$  as the linear combination  $-\alpha_{l+1}(V^l - V^{l+1}) + \beta_l(W^l + W^{l+1}) + (\alpha_l + \alpha_{l+1})(V^l + W^{l+1})$ .  $\square$

We will need currents with specified non-zero fluxes on the three sides at which cells join and zero flux on the other sides. The relevant sides were determined in Section 3.1; they are those which contain a vertex of  $G_0$ .

**Proposition 3.8.** *If  $I_j$ ,  $j = 0, N, 3N - 1$  satisfy  $\sum_{0, N, 3N-1} I_j = 0$  then there is a current  $J$  on  $F_n$  with flux  $I_j$  on  $L_j \cap F_n$  for  $j = 0, N, 3N - 1$  and zero on all other  $L_j \cap F_n$  and that has energy*

$$E_{F_n}(J, J) \leq \left( \frac{N^2}{4} E(V) + \frac{N^2}{18} (11N - 8) E(W) \right) \sum_{0, N, 3N-1} I_j^2 \leq \frac{11}{9} N^2 R_n \sum_{0, N, 3N-1} I_j^2$$

*Proof.* Write  $\Lambda'(N) = \{0, N, 3N - 1\}$ . Define coefficients  $\beta_j$  by

$$\beta_j = \begin{cases} I_N - I_{3N-1} & \text{if } j = 0 \\ I_{3N-1} - I_0 & \text{if } j = N \\ I_0 - I_N & \text{if } j = 3N - 1 \end{cases} \quad \beta_j = \begin{cases} 2I_N - 2I_0 & \text{if } 1 \leq j \leq N - 1 \\ 2I_{3N-1} - 2I_N & \text{if } N + 1 \leq j \leq 3N - 2 \\ 2I_0 - 2I_{3N-1} & \text{if } 3N \leq j \leq 4N - 1 \end{cases}$$

and let

$$J = -\frac{N}{2} \sum_{j \in \Lambda'} I_j V^j + \frac{N}{6} \sum_{j \in \Lambda} \beta_j W^j.$$

Then  $J$  is of the form  $\sum_j \alpha_j V^j + \beta_j W^j$  with  $\alpha_j = -\frac{N}{2} I_j$  for  $j \in \Lambda'$  and zero otherwise. One can verify the conditions of Lemma 3.7, so  $J$  is a current. Moreover, all of the  $W^j$  have zero flux through  $L_j \cap F_n$ , and  $V^j$  has flux  $-\frac{2}{N}$  through  $L_j \cap F_n$ , thus the flux of  $J$  is as stated.

By the orthogonality in Lemma 3.6 and (3.4),

$$E_{F_n}(J, J) = \frac{N^2}{4} E(V) \sum_{\Lambda'} I_j^2 + \frac{N^2}{36} E(W) \sum_{\Lambda} \beta_j^2.$$

It is straightforward to compute

$$\begin{aligned} \sum_{\Lambda} \beta_j^2 &= (4N - 3)(I_N - I_0)^2 + (8N - 7)(I_{3N-1} - I_N)^2 + (4N + 1)(I_0 - I_{3N-1})^2 \\ &= (16N - 9)I_0^2 + (20N - 17)I_N^2 + (20N - 13)I_{3N-1}^2 + 4(N - 1)I_0 I_N + 4(N - 2)I_0 I_{3N-1} \end{aligned}$$



where we used  $-2I_N I_{3N-1} = I_0^2 + I_N^2 + I_{3N-1}^2 + 2I_0 I_N + 2I_0 I_{3N-1}$ , which was obtained by squaring  $\sum_{\Lambda'} I_j = 0$ . Then the bound  $2I_0 I_j \leq \frac{3}{2}I_0^2 + \frac{2}{3}I_j^2$  for  $j = N, 3N - 1$  gives, also using  $N \geq 2$ ,

$$\sum_{\Lambda} \beta_j^2 \leq (22N - 18)I_0^2 + (22N - 19)I_N^2 + (22N - 16)I_{3N-1}^2.$$

This gives the energy estimate. The bound by  $R_n$  is from the expression following (3.4).  $\square$

Having established these results on currents, we turn to considering potentials, which will be built from the functions  $v^j$  and  $w^j$  so as to have specified boundary data at those  $C_j$  which are vertices of the graph  $D_0$  from Section 3.1.

**Lemma 3.9.** *The function  $v^1 + w^1 + v^0 - w^0$  extends continuously to  $F_n$ .*

*Proof.* In what follows we abuse notation to say a function is continuous on a union of the  $T_j$  if it has continuous extension to the closure of this union.

The proof uses the symmetries  $v^0(\bar{z}) = v^0(z)$  and  $w^0(\bar{z}) = -w^0(z)$ , which follow from Lemma 3.5 in the same manner as the proofs of (3.7) and (3.8). Note that  $z \mapsto \theta(\bar{z})$  is an isometry of  $T_0 \cup T_1$  and compute from the symmetries and (3.1) that

$$(3.9) \quad \begin{aligned} v^0(\theta(\bar{z})) &= v^0(\theta^{-1}(z)) = v^1(z), \\ w^1(\theta(\bar{z})) &= w^0(\bar{z}) = -w^0(z). \end{aligned}$$

Now observe that  $v^0 + w^1$  is continuous on  $T_0 \cup T_1$  because it is the restriction of the optimal potential  $u_n$  to this set, see (3.1). Using the preceding it follows that  $(v^1 - w^0)(z) = (v^0 + w^1)(\theta(\bar{z}))$  is also continuous, and thus  $v^1 + w^1 + v^0 - w^0$  is continuous on  $T_0 \cup T_1$ . What is more, we see that if  $z$  is in the common boundary of  $T_0$  and  $T_1$  then  $\theta(\bar{z}) = z$  and thus (3.9) gives  $w^1(z) = -w^0(z)$ . Continuity of  $v^0 + w^1$  at such points then implies  $v^0(z) = -w^0(z)$ , but this says  $v^0 + w^0$  vanishes identically on the common boundary of  $T_0$  and  $T_1$ . Thus  $v^1 + w^1 = v^0 + w^0 \circ \theta^{-1}$  vanishes on the common boundary of  $T_1$  and  $T_2$ , and  $(v^0 - w^0)(z) = (v^0 + w^0)(\bar{z})$  vanishes on the common boundary of  $T_0$  and  $T_{-1}$ . Together these show  $v^1 + w^1 + v^0 - w^0$  vanishes on the boundary of  $T_0 \cup T_1$  in  $F_n$ , completing the proof.  $\square$

**Proposition 3.10.** *Given a function  $u$  on  $D_0$  that is harmonic at 0 there is a potential  $f$  on  $F_n$  with  $f(C_j) = u(C_j)$  for  $C_j \in D_0$  and*

$$\mathcal{E}_{F_n}(f, f) \leq (\mathcal{E}_n(v) + \mathcal{E}_n(w)) \sum_{C_j \in D_0} (u(C_j) - u(0))^2 = \frac{2}{N} R_n^{-1} \sum_{C_j \in D_0} (u(C_j) - u(0))^2.$$

*If  $f(C_{j+1}) = f(C_j)$  for some  $j \in \{0, N, 3N - 1\}$  then  $f$  is constant on the edge  $L_j \cap F_n$ .*

*Proof.* Let  $z_j = u(C_j) - u(0)$  for  $C_j \in D_0$  and  $z_j = 0$  otherwise. With indices modulo  $4N$ , define

$$f = u(0) + \frac{1}{2} \sum_{j \in \Lambda(N)} z_j (w^{j-1} - v^{j-1} - v^j - w^j) = u(0) + \frac{1}{2} \sum_j (z_{j+1} - z_j) w^j - (z_{j+1} + z_j) v^j.$$

This is continuous on  $F_n$  because it is a linear combination of rotations of the function in Lemma 3.9. Recall from Section 2.2 that a function is a potential if it is continuous and in the Sobolev space  $H^1$ . Since  $v^j$  and  $w^j$  are restrictions of Sobolev functions to the domains  $T_j$ , it is standard that a linear combination which extends to be continuous on  $\cup_j T_j$  is Sobolev on  $\cup_j T_j$ ; for example it follows immediately from the characterization of  $H^1$  using absolute continuity on lines, see [9, Theorem 2.1.4]. We therefore conclude that  $f$  is a potential. Using  $w^{j-1}(C_j) = 1$ ,  $v^{j-1}(C_j) = w^{j-1}(C_j) = w^j(C_j) = -1$  and  $v^l(C_j) = w^l(C_j) = 0$  for  $l \neq j, j + 1$  we easily see  $f(C_j) = u(C_j)$  for  $C_j \in D_0$ .

From the orthogonality in Lemma 3.6 and (3.3) we have

$$\mathcal{E}_{F_n}(f, f) = \frac{1}{4}\mathcal{E}_n(v) \sum_{j \in \Lambda''' } (z_{j+1} + z_j)^2 + \frac{1}{4}\mathcal{E}_n(w) \sum_{j \in \Lambda''' } (z_{j+1} - z_j)^2 \leq (\mathcal{E}_n(v) + \mathcal{E}_n(w)) \sum_j z_j^2$$

where we used  $(z_{j+1} \pm z_j)^2 \leq 2z_{j+1}^2 + 2z_j^2$ . The remaining part of the asserted energy bound is from from (3.5).

Finally, suppose there is  $j \in \{0, N, 3N - 1\}$  for which  $f(C_{j+1}) = f(C_j)$ . Then  $z_{j+1} = z_j$ , and on the edge  $L_j \cap F_n$  we have  $f = u(0) - (z_{j+1} + z_j)v^j$ . However (3.1) says  $v^j$  comes from the restriction of  $u_n$  to  $L_0$ , where  $u_n \equiv 1$ , so  $v^j$  is constant on  $L_j \cap F_n$  and so is  $f$ .  $\square$

#### 4. BOUNDS

Our main resistance estimate is obtained from the results of the previous sections by constructing a feasible current and potential on  $F_{m+n}$ . We use the optimal current on  $G_m$  and optimal potential on  $D_m$  to define boundary data on  $m$ -cells that are copies of  $F_n$ , and then build matching currents and potentials from Propositions 3.8 and 3.10 to prove the following theorem.

**Theorem 4.1.** *For  $n \geq 0$  and  $m \geq 1$*

$$\frac{9}{44N}R_0^{-1}R_nR_m \leq R_{m+n} \leq \frac{44N}{9}R_0^{-1}R_nR_m.$$

*Proof.* For fixed  $m \geq 1$  let  $\tilde{I}_m^G$  be the optimal current on the graph  $G_m$  and  $\tilde{u}_m^D$  be the optimal potential on the graph  $D_m$ , both for the sets  $A_m$  and  $B_m$ . Recall that for each cell we have an address  $w = w_1 \cdots w_m$  and a map  $\psi_w$  as in Section 3.1 so that  $\tilde{I}_m^G \circ \psi_w$  is a current on  $G_0$  and  $\tilde{u}_m^D \circ \psi_w$  is a potential on  $D_0$ .

Now fix  $n \geq 0$  and consider  $F_{m+n}$ . Then  $\psi_w$  maps  $F_n$  to the  $m$ -cell of  $F_{m+n}$  with address  $w$ , and we write  $J_w$  for the current from Proposition 3.8 with fluxes from  $\tilde{I}_m^G \circ \psi_w$  and  $f_w$  for the potential from Proposition 3.10 with boundary data from  $\tilde{u}_m^D \circ \psi_w$ . In particular, summing over all words of length  $m$  we have from these propositions and the optimality of the current and potential that

$$(4.1) \quad E_{F_{m+n}}\left(\sum_w J_w, \sum_w J_w\right) = \sum_w E_{F_n}(J_w, J_w) \leq \frac{11}{9}N^2R_nE_{G_m}(\tilde{I}_m^G, \tilde{I}_m^G) = \frac{11}{9}N^2R_nR_m^G$$

$$(4.2) \quad \mathcal{E}_{F_{m+n}}\left(\sum_w f_w, \sum_w f_w\right) = \sum_w \mathcal{E}_{F_n}(f_w, f_w) \leq \frac{2}{N}R_n^{-1}\mathcal{E}_{D_m}(\tilde{u}_m^D, \tilde{u}_m^D) = \frac{2}{N}R_n^{-1}(R_m^D)^{-1}.$$

Since  $\tilde{I}_m^G$  is a current, its flux through the edges incident at a non-boundary point is zero. Using this fact at the vertex on the center of a side where two  $m$ -cells meet we see that the net flux of  $\sum_w J_w$  through such a side is zero. Moreover, in  $\sum_w J_w$  the flux through this side is a (scaled) copy of  $v^j$  from (3.1). Using the fact that  $v^j$  is a rotate of  $v^0$  and  $v^0(\bar{z}) = v^0(z)$ , we see that all the fluxes are multiples of a single vector field, and thus the cancellation of the net flux guarantees cancellation of the fluxes themselves. By the same argument used in proving Lemma 3.7 we conclude that  $\sum_w J_w$  is a current on  $F_{m+n}$ . Its net flux through a boundary edge is the same as that of  $\tilde{I}_m^G$ , so is  $-1$  through  $A_{m+n}$  and  $1$  through  $B_{m+n}$ . Hence  $\sum_w J_w$  is a feasible current from  $A_{m+n}$  to  $B_{m+n}$  on  $F_{m+n}$ , and (4.1) together with Theorem 2.3 implies

$$(4.3) \quad R_{m+n} \leq E_{F_{m+n}}\left(\sum_w J_w, \sum_w J_w\right) \leq \frac{11}{9}N^2R_nR_m^G.$$

Similarly, we can see that  $\sum_w f_w$  extends by continuity to give a potential on  $F_{m+n}$ . Each side where two  $m$ -cells meet is the line segment at the intersection of the closures of copies of triangles  $T_j$  and  $T_{j'}$  under maps  $\psi_w, \psi_{w'}$  corresponding to the  $m$ -cells. Extending  $\sum_w f_w$  to the closure of each of these triangles we see it coincides with  $\tilde{u}_m^D$  at the endpoints of this line segment, while along the line it is a linear combination of  $v^j$  and  $w^j$  as in Proposition 3.10. This linear combination

depends only on the endpoint values, so is the same on the line from  $\psi_w(T_j)$  as on the line from  $\psi_{w'}(T_{j'})$ , showing that  $\sum_w f_w$  has continuous extension to  $F_{m+n}$ . Since  $\tilde{u}_m^D$  is 0 at all endpoints of sides of cells in  $A_{m+n}$  and 1 at all endpoints of sides in  $B_{m+n}$ , the final result of Proposition 3.10 ensures  $\sum_w f_w$  has value 0 on  $A_{m+n}$  and 1 on  $B_{m+n}$ , so is a feasible potential. Combining this with (4.2) and (2.2) gives

$$(4.4) \quad R_{m+n}^{-1} \leq \mathcal{E}_{F_{m+n}} \left( \sum_w f_w, \sum_w f_w \right) \leq \frac{2}{N} R_n^{-1} (R_m^D)^{-1}.$$

Our estimates (4.3) and (4.4), together with Lemma 3.3, give for  $n \geq 0$ ,  $m \geq 1$  that

$$\frac{N}{2} R_n R_m^D \leq R_{m+n} \leq \frac{11}{9} N^2 R_n R_m^G = \frac{22}{9} N^2 R_n R_m^D.$$

In particular, for  $n = 0$  we have  $R_m^D \leq \frac{2}{N} R_0^{-1} R_m$  and  $\frac{9}{22N^2} R_0^{-1} R_m \leq R_m^D$ , which may be substituted into the previous expression to obtain the theorem.  $\square$

#### REFERENCES

- [1] Ulysses A. IV Andrews. *Existence of Diffusions on  $4N$  Carpets*. PhD thesis, University of Connecticut, 2017. <https://opencommons.uconn.edu/dissertations/1477>.
- [2] M. T. Barlow and R. F. Bass. On the resistance of the Sierpiński carpet. *Proc. Roy. Soc. London Ser. A*, 431(1882):345–360, 1990.
- [3] M. T. Barlow, R. F. Bass, and J. D. Sherwood. Resistance and spectral dimension of Sierpiński carpets. *J. Phys. A*, 23(6):L253–L258, 1990.
- [4] Russell Brown. The mixed problem for Laplace’s equation in a class of Lipschitz domains. *Comm. Partial Differential Equations*, 19(7-8):1217–1233, 1994.
- [5] Peter G. Doyle and J. Laurie Snell. *Random walks and electric networks*, volume 22 of *Carus Mathematical Monographs*. Mathematical Association of America, Washington, DC, 1984.
- [6] Lawrence C. Evans and Ronald F. Gariepy. *Measure theory and fine properties of functions*. Studies in Advanced Mathematics. CRC Press, Boca Raton, FL, 1992.
- [7] Pierre Grisvard. *Elliptic problems in nonsmooth domains*, volume 69 of *Classics in Applied Mathematics*. Society for Industrial and Applied Mathematics (SIAM), Philadelphia, PA, 2011.
- [8] John E. Hutchinson. Fractals and self-similarity. *Indiana Univ. Math. J.*, 30(5):713–747, 1981.
- [9] William P. Ziemer. *Weakly differentiable functions*, volume 120 of *Graduate Texts in Mathematics*. Springer-Verlag, New York, 1989. Sobolev spaces and functions of bounded variation.

CLAIRE CANNER, ROCHESTER INSTITUTE OF TECHNOLOGY

*Email address:* `clairemcanner@gmail.com`

CHRISTOPHER HAYES, DEPARTMENT OF MATHEMATICS, UNIVERSITY OF CONNECTICUT, STORRS, CT 06269-1009, U.S.A.

*Email address:* `christopher.k.hayes@uconn.edu`

SHINYU HUANG, WILLIAMS COLLEGE

*Email address:* `wsh1@williams.edu`

MICHAEL ORWIN, KALAMAZOO COLLEGE

*Email address:* `orwinmc@gmail.com`

LUKE G. ROGERS, DEPARTMENT OF MATHEMATICS, UNIVERSITY OF CONNECTICUT, STORRS, CT 06269-1009, U.S.A.

*Email address:* `luke.rogers@uconn.edu`